

Parameter dependency of pinch in toroidal momentum transport of tokamaks

S.M. Yang, D.H. Na and Yong-Su Na

Department of Nuclear Engineering, Seoul National University, Seoul 151-744, Korea

Abstract – The toroidal momentum transport in tokamak plasmas is studied using quasilinear gyrokinetic calculation. An inward convection of toroidal momentum, momentum pinch, is investigated in various plasma parameters. A particular focus is given to the effect of change of the dominant micro-instability in a plasma due to change of those plasma parameters to the pinch term. The calculation is done with electrostatic GKW code to identify the characteristics of the dominant micro-instabilities which dominate in a plasma.

I. INTRODUCTION

Understanding of plasma rotation is important issue since the rotation and its shear can contribute to the enhancement of the confinement and stabilization of MHD instability such as RWM and NTM [1, 2, 3]. Especially for the future tokamak like ITER, the externally injected torque will be small. Interestingly, it has been observed that the plasma rotation can have substantial level even without the externally applied torque such as neutral beam injection. Based on the idea, it has been found that the radial transport of toroidal rotation can be driven by non-diffusive transport other than a plasma viscosity. A momentum transport property in the toroidal momentum equation can be described as the Toroidal Reynolds stress. The Toroidal Reynolds stress can be expressed as summation of diffusive term, pinch term, and residual stress term respectively [4],

$$\Pi_\phi = -\chi_\phi \frac{\partial L_\phi}{\partial r} + V_\phi L_\phi + \Pi_{res} \quad (1)$$

Various studies have been carried out for the intrinsic toroidal rotation and the toroidal momentum pinch in experiment and theory.

Theoretically, the pinch term is known to depend on plasma parameters such as magnetic field inhomogeneity, density gradient, ratio of electron and ion temperature and so on [5 - 10]. In this work, we consider various plasma parameters and equilibria to investigate their influence on the pinch term. Particularly, the effect of change of the dominant micro-instability in a plasma due to change of those plasma parameters is investigated. Linear electrostatic gyrokinetic calculation is done with GKW code to identify the characteristics of the dominant micro-instabilities. In Sec. II a brief description of the numerical simulation is shown. In Sec. III momentum pinch is studied in various equilibrium condition and dominant micro-instability changes are studied. Conclusions are drawn in Sec. IV.

II. DESCRIPTION OF THE ACTUAL WORK

1. Parameter scan choices

Various range of the normalized logarithmic gradient R/L_T is possible during the plasma operation. This can be changed by the localized external actuator or by the enhancement of the confinement properties. In previous study, parametric scans are conducted with respect to R/L_{Ti} , R/L_n and collisionality in the presence of trapped electron mode [11]. Here, change of R/L_{Te} is studied which is more likely to be experimentally relevant parameter due to electron Cyclotron Heating (ECH). ECH is one of the popular methods of localized heating in tokamak which can increase the electron temperature gradient while keeping other parameters. The effect of ECH to the rotation profile is observed in the experiments in KSTAR [12, 13] and ASDEX-U [14]. The change of the dominant micro-instability from ITG to TEM can occur with the increase of R/L_{Te} . In addition, effect of R/L_{Ti} , T_e/T_i and R/L_n at different safety factor q is investigated where the safety factor can be changed by the toroidal magnetic field and plasma current or by the plasma shape.

2. Calculation of pinch number using GKW

Momentum pinch, driven by turbulent equipartition convective velocity and curvature can be calculated using GKW [15] by solving the kinetic Vlasov equation averaged over fast gyro-motion. The physics of the plasma motion has been implemented through a formulation of the gyro-kinetic equation in the co-moving system [6]. Using GKW, the estimation of momentum pinch to viscosity ratio RV_ϕ/χ_ϕ in various plasma parameters can be investigated. The transition from ITG to TEM can be tracked by the sign of the real frequency of the most unstable mode ω_r where it is positive for ITG and negative for TEM in simulations. The parameter scan is conducted by keeping all other parameters at standard ITG case [16] where $R/L_{Te} = 9$, $R/L_{Ti} = 9$, $R/L_n = 3$, safety factor $q = 2$, magnetic shear = 1 and poloidal wave number $k_\theta \rho_s = 0.3$ and $\epsilon = 0.35$ is used.

In order to determine the both Prandtl number (χ_ϕ/χ_i) and pinch number (RV_ϕ/χ_ϕ), two simulations are executed. Based on the assumption that the fluxes are linear in both v_ϕ and ∇v_ϕ , Prandtl number and pinch number can be obtained.

The assumption is well satisfied as shown in Ref. [6]. In the simulation with zero rotation, momentum flux gives information on the viscosity. Another simulation with zero gradient gives the contribution of the momentum pinch, since the diagonal contribution is zero in this case. There is no contribution of Residual stress (Π_{res}) to the momentum flux when zero rotation and zero rotation gradient is used. Extra symmetry breaking, for example from ExB shearing, can contain residual stress driven momentum flux but that is not included in this calculation.

III. RESULTS

The momentum flux can be represented as follows.

$$\Gamma_\phi = \langle \int d^3v \mathbf{v} v_E m v_{\parallel} f \rangle \quad (2)$$

For $u = 0$ and $u' = 0$ case, momentum flux is zero in this simulation. This confirms the previous statement that there is no contribution of Residual stress in this study. The results can be explained by the combination with the parallel velocity fluctuation and fluctuating ExB velocity as shown in Figure 1. Electric potential is symmetric as shown in Figure 1 (a), while the velocity fluctuation is antisymmetric with respect to the low field side position $\theta/2\pi = 0$. Taking the flux surface average gives the zero momentum flux in this case as discussed in previous studies [17].

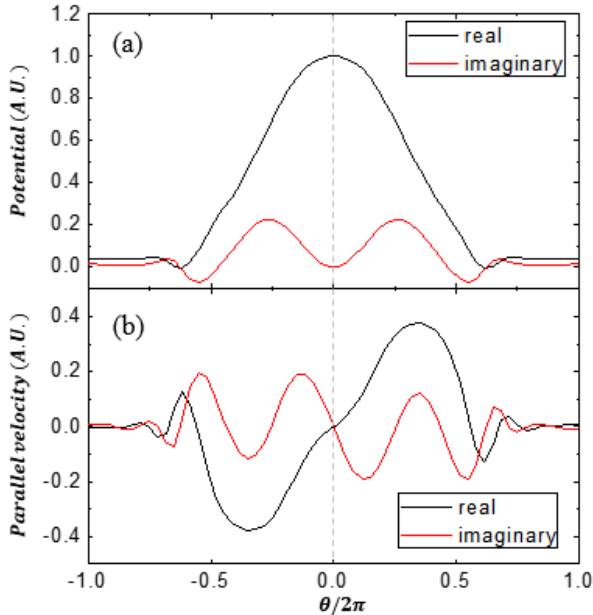


Fig. 1. Mode structure along the field line at $u = 0$. (a) Real part of the perturbed potential (black) and imaginary part of the perturbed potential (red). (b) Real part of the perturbed parallel flow velocity (black) and imaginary part of the perturbed parallel flow velocity (red).

When finite velocity $u = 0.3$ is considered, finite momentum flux can be obtained with broken symmetry in the mode structure as shown in Fig 2. This broken symmetry drives the finite momentum pinch with flux surface average in the presence of the kinetic electron [17].

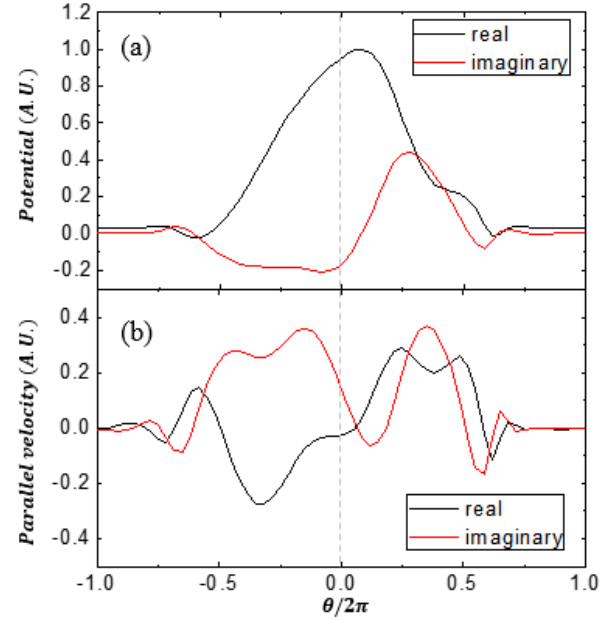


Fig. 2. Mode structure along the field line at $u = 0.3$. (a) Real part of the perturbed potential (black) and imaginary part of the perturbed potential (red). (b) Real part of the perturbed parallel flow velocity (black) and imaginary part of the perturbed parallel flow velocity (red).

A dependence on the temperature ratio T_e/T_i is investigated in each dominant mode. Strong ITG case ($R/L_{Ti} = 12$ $R/L_{Te} = 3$), standard ITG case ($R/L_{Ti} = 9$ $R/L_{Te} = 9$) and TEM case ($R/L_{Ti} = 12$ $R/L_{Te} = 3$) are compared respectively in Fig. 3. A dependence is investigated in various safety factor 0.5, 1 and 2. In general, the decrease of RV_ϕ/χ_ϕ is observed at $q = 1$ and $q = 2$ as T_e/T_i increases. This is consistent with analytic studies in ITG [9, 10]. This trend changes when TEM is dominant at $q = 0.5$. An increase of RV_ϕ/χ_ϕ is observed with respect to T_e/T_i . This trend is similar to the trend observed in Ref. 11 where the sign reversal of ω_r from ITG to TEM leads to the opposite behavior with respect to T_e/T_i at $R/L_n = 1$ at $q = 2$. As discussed in Ref. 18, effect of safety factor in ITG can be explained by the relation between mode localization and safety factor. As safety factor decreases, mode is less localized and the decrease of the momentum pinch is observed. The result in TEM case shows that this trend could be different in TEM dominant case.

The effect of a transition from ITG to TEM modes can be explored by various logarithmic gradient. The transition is investigated in different safety factor. Change of RV_ϕ/χ_ϕ

with respect to R/L_{Te} is shown in Fig. 4. In ITG, contribution of R/L_{Te} to RV_{ϕ}/χ_{ϕ} is small. However, after the change of the dominant micro-instability, clear change of RV_{ϕ}/χ_{ϕ} is found. At $q = 2$, the decrease of RV_{ϕ}/χ_{ϕ} is observed during the mode transition. On the contrary, at $q = 1$, the increase of RV_{ϕ}/χ_{ϕ} is observed. This shows that the RV_{ϕ}/χ_{ϕ} change during mode transition depends largely on the safety factor q .

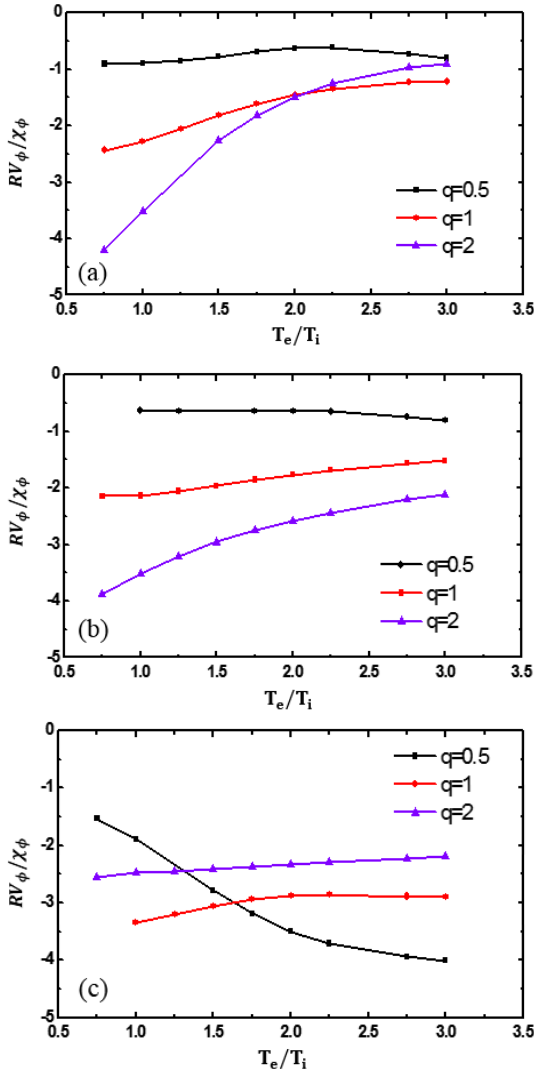


Fig. 3. Momentum pinch to viscosity ratio RV_{ϕ}/χ_{ϕ} as a function of the electron to ion temperature ratio T_e/T_i for $q = 0.5$ (black), $q = 1$ (red), and $q = 2$ (violet) in strong ITG case (a), standard ITG case (b) and TEM case.

Dependence of R/L_{Ti} is also explored. With the change of the R/L_{Ti} , variation of RV_{ϕ}/χ_{ϕ} is observed in both $q = 1$ and $q = 2$ as shown in Fig. 5. When R/L_{Ti} increases, RV_{ϕ}/χ_{ϕ} increases in ITG. Change of RV_{ϕ}/χ_{ϕ} with respect to R/L_{Ti} is observed in the TEM case as well while

contribution of R/L_{Te} to ITG is very small in the R/L_{Te} scan. This tells the R/L_{Ti} contribution to TEM driven momentum pinch is not negligible. It is interesting to see that R/L_{Ti} dependence to momentum pinch reverses at different safety factor. Also, as it is observed in R/L_{Te} scan, RV_{ϕ}/χ_{ϕ} change during ITG to TEM transition is different between at $q = 2$ and $q=1$ as shown in Fig. 5.

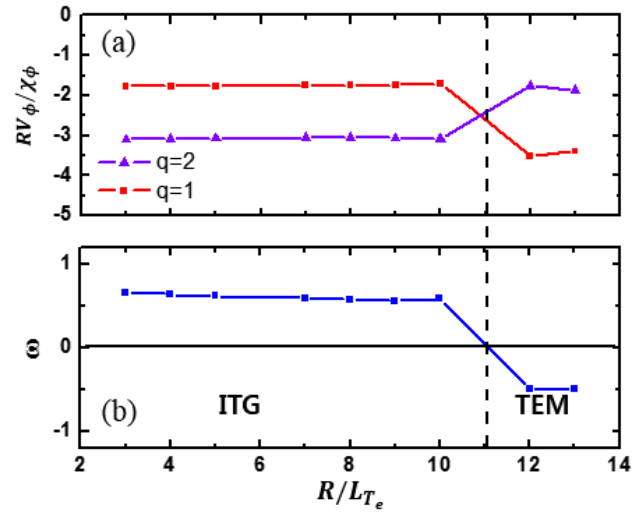


Fig. 4. Momentum pinch to viscosity ratio RV_{ϕ}/χ_{ϕ} at safety factor $q = 1$ (red) and $q = 2$ (violet) (a) and real frequency ω of unstable mode (b) as a function of the normalized logarithmic R/L_{Te} at transition from a dominant ITG to a dominant TEM instability.

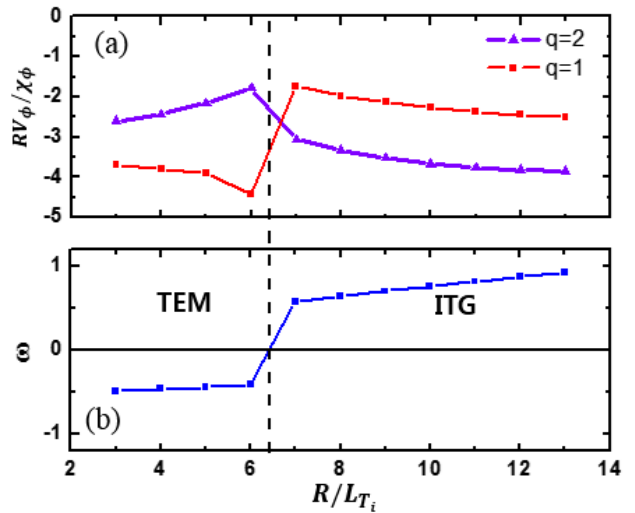


Fig. 5. Momentum pinch to viscosity ratio RV_{ϕ}/χ_{ϕ} at safety factor $q = 1$ (red) and $q = 2$ (violet) (a) and real frequency ω of unstable mode (b) as a function of the normalized logarithmic R/L_{Ti} at transition from a dominant TEM to a dominant ITG instability.

Change of R/L_n can also trigger mode transition in marginal case. As marginal cases, $R/L_{Ti} = 6, R/L_{Te} = 6$ at $q = 2$ and $R/L_{Ti} = 6, R/L_{Te} = 4$ at $q = 1$ are in Fig. 6. Unlike R/L_{Ti} and R/L_{Te} dependence, safety factor seems to have no contribution when dominant micro instability changes from ITG to TEM with R/L_n change. From this, R/L_n driven momentum pinch seems to have a similar effect in both ITG and TEM.

Based on the result, safety factor dependence of RV_ϕ/χ_ϕ in ITG and TEM is calculated and demonstrated in Fig. 7. The dependence shows that the direction of RV_ϕ/χ_ϕ change during the mode transition depends on safety factor. The trend changes at $q = 1.4$ and change of RV_ϕ/χ_ϕ is not expected even with a change of the dominant micro-instability at $q = 1.4$ from the simulations. This occurs because the TEM driven momentum pinch has non-monotonic dependence on safety factor as shown in Fig. 7. Because it is more difficult to conduct analytic estimation in TEM case, this tells the necessity of gyrokinetic simulation especially when different equilibrium conditions are applied.

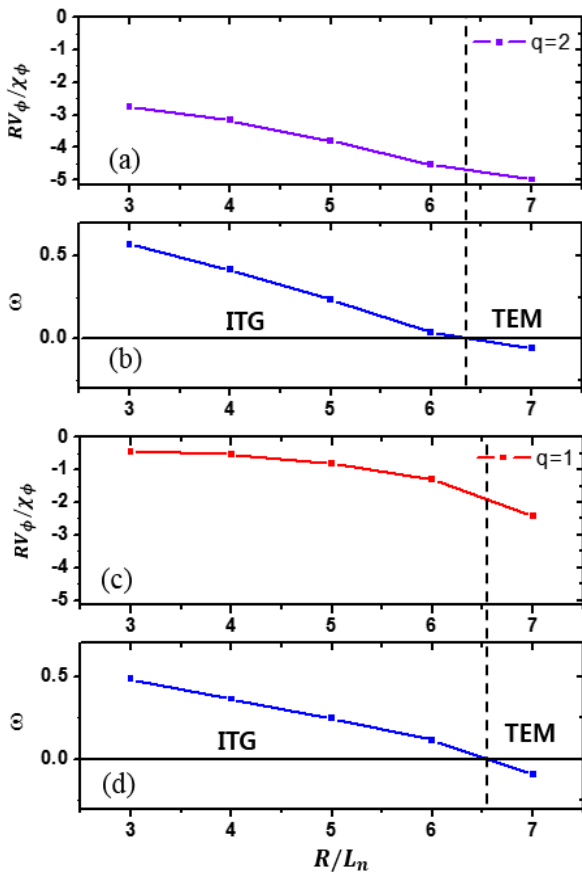


Fig. 6. Momentum pinch to viscosity ratio RV_ϕ/χ_ϕ at safety factor (a) and real frequency ω of unstable mode (b) as a

function of the normalized logarithmic R/L_n at $q = 2$ and (c) and real frequency ω of unstable mode (d) as a function of the normalized logarithmic R/L_n at $q = 1$ at transition from a dominant TEM to a dominant ITG instability.

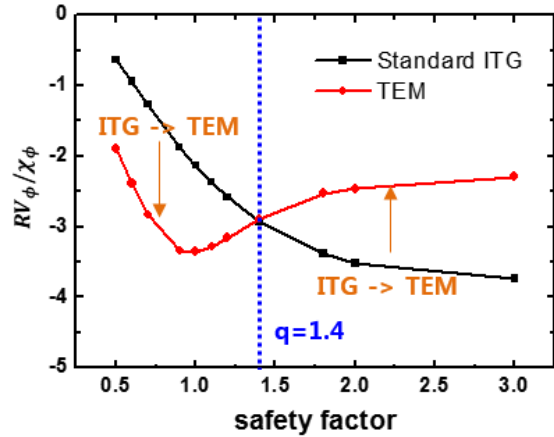


Fig. 7. Momentum pinch to viscosity ratio RV_ϕ/χ_ϕ as a function of the safety factor q for the standard ITG case (black) and the TEM case (red).

Another geometric factor, magnetic shear, is also investigated. Change of RV_ϕ/χ_ϕ with respect to magnetic shear is shown in Fig. 8 at $q = 2$. For magnetic shear, non-monotonic dependence of momentum pinch in ITG case is observed while it is linearly proportional to magnetic shear in TEM case in $q = 2$. This also leads to another interesting case where the direction of momentum pinch at with dominant mode change reverses. In here, when $q = 2, s = 1.3$, change of RV_ϕ/χ_ϕ is not expected even with a change of the dominant micro-instability as shown in Fig. 7. Depending on the magnetic shear, dominant mode transition could have different effect to the rotation profile which is similar to the observation at safety factor scan.

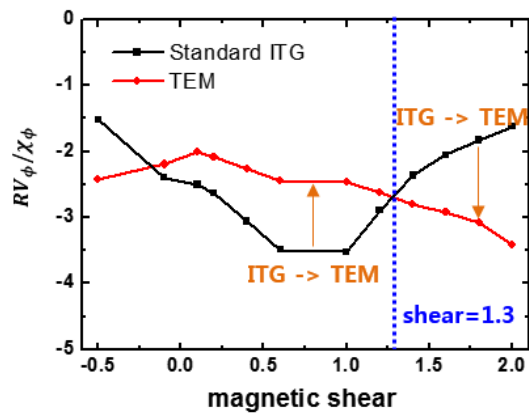


Fig. 8. Momentum pinch to viscosity ratio RV_ϕ/χ_ϕ as a function of the magnetic shear s for the standard ITG case (black) and the TEM case (red).

IV. CONCLUSIONS AND DISCUSSION

Using GKW simulation, the physical investigation of the transport of toroidal momentum pinch in the presence of TEM and ITG instabilities are investigated. The result can be used for practical application for the experimental validation of the theory of the momentum pinch.

The result shows that the momentum pinch is highly sensitive to the equilibrium condition. It has been found that the ratio of the momentum pinch to the toroidal viscosity is found to increase or decrease depending on the safety factor or magnetic shear. When the drive of the TEM is density gradient, this trend is not observed and temperature drive seems to be relevant for the trend. This is due to the non-monotonic dependence of safety factor and magnetic shear to momentum pinch as it is estimated from linear gyrokinetic simulation.

For reliable prediction of the plasma rotation, understanding of the physics of the toroidal momentum pinch is required. Based on the study, theoretical prediction can be applied for the design of dedicated experiments for theory validation.

NOMENCLATURE

L_ϕ = Toroidal angular momentum
 Π_ϕ = Turbulent Reynolds stress
 χ_ϕ = Momentum diffusivity term
 V_ϕ = Momentum pinch term
 Π_{res} = Residual stress term
 $\langle \ \rangle$ = Flux surface average
 \mathbf{v}_E = fluctuating ExB velocity
 f = perturbed distribution function
 ϵ = Aspect ratio
 q = Safety factor

ENDNOTES

REFERENCES

1. T.S. Hahm et al., Phys. Plasmas **1**, 2940 (1994)
2. L.-J. Zheng et al., PRL **95**, 255003 (2005)
3. R. J. Buttery et al., PHYSICS OF PLASMAS **15**, 056115 (2008)
4. P.H. Diamond et al., Nucl. Fusion **49**, 045002 (2009).
5. T.S. Hahm et al., Physics of Plasmas **14**, 072302 (2007)
6. A.G. Peeters et al., Physical Review Letters **98**, 265003 (2007)
7. T. S. Hahm et al., Phys. Plasmas **15**, 055902 (2008)
8. T. S. Hahm et al., Phys. Plasmas **16**, 034704 (2009)
9. A.G. Peeters et al., Phys. Plasmas **16**, 042310 (2009)

10. E.S. Yoon and T.S. Hahm, Nucl. Fusion **50**, 064006 (2010)
11. Kluy et al., Phys. Plasmas **16**, 122302 (2009)
12. J. Seol et al., PRL **109**, 195003 (2012)
13. Y.J. Shi et al., Nucl. Fusion **53**, 113031 (2013)
14. R M McDermott et al., Plasma Phys. Control. Fusion **53** 035007 (2011)
15. A.G. Peeters, et al., Computer Physics Communications, **180**, 2650 (2009)
16. R.E. Waltz et al., Phys. Plasmas **4**, 2482 (1997)
17. A.G. Peeters et al., Phys. Plasmas **16**, 062311 (2009)
18. A.G. Peeters et al., Nucl. Fusion **51**, 094027 (2011)